iJRASET
International Journal For Research in Applied Science and Engineering Technology

# INTERNATIONAL JOURNAL FOR RESEARCH

IN APPLIED SCIENCE & ENGINEERING TECHNOLOGY

**Volume:** 6 **Issue:** III **Month of publication:** March 2018

**DOI:** http://doi.org/10.22214/ijraset.2018.3133

www.ijraset.com

Call: 08813907089 | E-mail ID: ijraset@gmail.com

International Journal for Research in Applied Science & Engineering Technology (IJRASET)
*ISSN: 2321-9653; IC Value: 45.98; SJ Impact Factor: 6.887*
*Volume 6 Issue III, March 2018- Available at www.ijraset.com*

# Luminescent Activator $Dy^{3+}$ Ion in Auto-Combusted Nanosized La $(OH)_3$

V Anslin Ferby[1,2], M Bououdina[3], A Moses Ezhil Raj[1,2]
[1]*Department of Physics and Research Centre, Scott Christian College (Autonomous) Nagercoil - 629003, INDIA*
[2]*Manonmaniam Sundaranar University, Abishekapatti, Tirunelveli-627012*
[3]*Department of Physics, College of Science, University of Bahrain, P.O Box 32038, Kingdom of Bahrain*

***Abstract:*** ***Nanocrystalline lanthanum hydroxide powder was prepared by auto-combustion method using high purity lanthanum nitrate as oxidant and citric acid as fuel. Dysprosium doped Lanthanum hydroxide nano particles were prepared by mixing lanthanum nitrate and dysprosium nitrate for three different doping concentrations 2, 5 and 10 wt. %. From the X-ray diffraction peaks, it can be confirmed that the obtained samples have polycrystalline structures, and are perfectly indexed to the hexagonal crystals of La(OH)3 [space group: P63/m (176)] based on the JCPDS standards (JCPDS cards (No. 36-1481). The optical absorption spectra of pure and Dy3+ doped La(OH)3 nano powders have been recorded to understand the type of optical transition and to estimate the optical band gap energy. The optical band gap variations with dopant concentration were discussed. Dy3+ in La(OH)3 host lattice emits light from blue to red region. The luminescence comes from the 4F9/2 level of dysprosium. The most intensive is a yellow greenish emission, which is assigned to the 4F9/2 →6H13/2 transition.***
***Keywords: Combustion synthesis, nanopowders, X-ray diffraction, Photoluminescence, Lifetime***

## I. INTRODUCTION

Usually materials that absorb energy and subsequently emit it as ultra-violet, visible or infra red light are defined as phosphors. They are usually composed of a transparent host material doped with activator ions, typically a rare earth (RE) or transition metal. In particular, RE-doped phosphors are important materials having significant applications in artificial light; X-ray medical radiography; plasma, vacuum fluorescent and field emission displays; high-power solid-state lasers and cathode-ray tubes because of its peculiar electronic, optical, and chemical characteristics resulting from their unique 4f electron configuration [1-3].

Because of similar electronic configuration and size of the dopant lanthanide atoms, rare-earth sesquioxides behaves as host materials having an excellent chemical stability, broad transparency range, better thermal conductivity and high light output [4]. Because of identical ionic radii [5], electronic structures and electro-negativity [6] of host lanthanide ions, it can be easily replaced by luminescence-active $RE^{3+}$ ions (e.g. $Ho^{3+}$, $Yb^{3+}$, $Dy^{3+}$, $Tm^{3+}$, $Eu^{3+}$, $Er^{3+}$, or $Sm^{3+}$) in a wide range of concentrations, without considerably degrading the lattice structure.

For doping with these $RE^{3+}$ ions, $La(OH)_3$ serve as a host because of its unique characteristics such as its large band gap of 4.3 eV, excellent stability, similar ionic radius to that of several RE ions, long lifetime luminescence and low phonon energy (~400 $cm^{-1}$) [7, 8], which result in high up-conversion (UC) photoluminescence (PL) properties [9], and exhibits brighter luminescence than the purr $La(OH)_3$.

The emission from the $RE^{3+}$ dopant is mainly due to the electric and magnetic dipole optical transitions based on their unique intra-4f transitions, which are shielded by the outer 5s and 5p orbitals, consequently, leading to sharp emissions and narrow bands. Hexagonal $La(OH)_3$ with space group P63/m (No. 176) and the polyhedrons around $La^{3+}$ and La-O bonds in the structures is presented in Fig. 1.

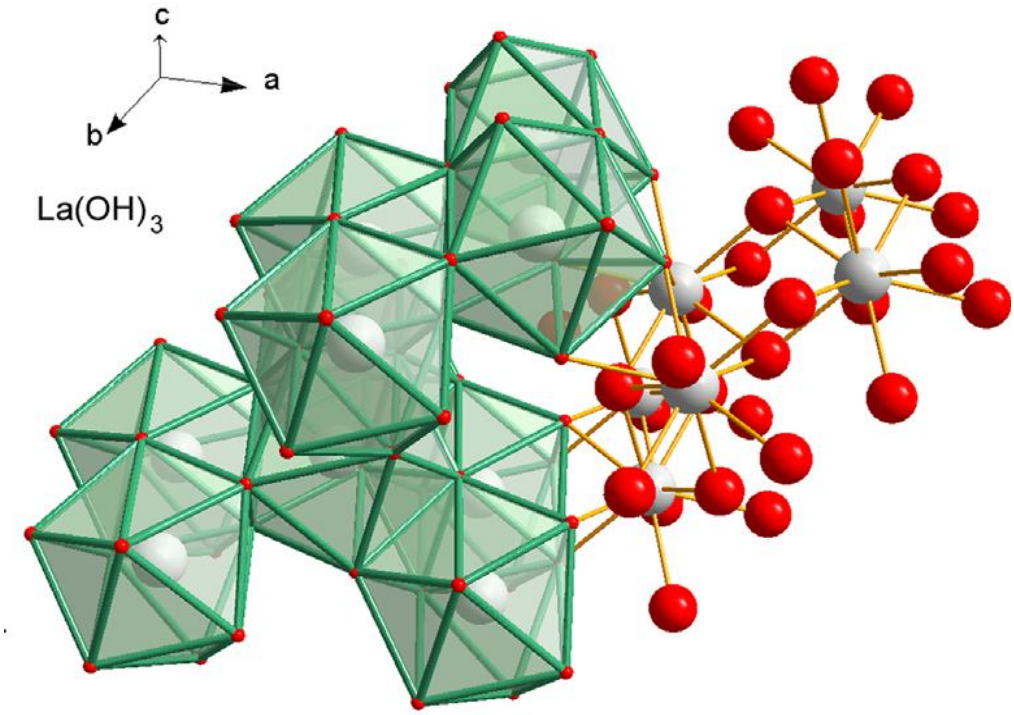


Fig. 1 Crystal structure of $La(OH)_3$

Generally, luminescence types can be classified as: down-conversion luminescence (DCL) and up-conversion luminescence (UCL). DCL is typical Stokes emission process under UV or electron beam (high energy) direct excitation (absorbing a short wavelength light and releasing long-wavelength emission through the dopant ions), while UCL is well known as anti-Stokes emission process under NIR or infrared light excitation (absorbs two or more low energy photons and releases a high-energy luminescence photon [10, 11]. The former is mainly applied in lighting and display fields like cathode ray tubes (CRTs), plasma display panels (PDPs), filed emission displays (FEDs) and so on. The latter has several advantages in the field of biomedicine [12]. However, the efficiency of the fabricated device depends strongly on the material chemical composition, crystal structure, shape, and dimensionality of the host material which are sensitive to the bonding states of rare earth ions.

The up-conversion efficiency depends on host matrix, the dopant concentration, energy migration between the active ions and the statistical distributions of active ions, and site symmetry of the active ions in the host matrix. With the suitable selection of host matrix and RE dopant ion concentration, the up-conversion performance of the material could be significantly enhanced. Moreover, the relatively low phonon energy host enables high UCL efficiency in $RE^{3+}$ ions by efficiently hindering non-radiative losses [13]. Thus, $La(OH)_3$ is an ideal host for design of up-conversion luminescence.

Moreover, resolution is a pivotal index for display, which is closely related to the particle size of the phosphors and thus smaller particles are propitious to higher resolution. For conventional powder phosphors, a reduction in the particle size is achieved by mechanically grinding techniques. This mechanically grinding method easily results in forming large amount of surface defects, which provide non-radiative recombination process, and ultimately degrade the luminescent efficiency. Therefore, the direct preparation of luminescent materials in nanoscale has become vital [14]. Since nanoparticles synthesized via the combustion technique are usually pure and defect free, they can be used as powder phospers on doping with RE ions.

Trivalent rare-earth (RE) ions are the suitable candidates for the UCL processes due to their abundant energy levels and narrow emission spectral lines [15, 16]. In the present study, $La(OH)_3$ is chosen as an ideal host material for various phosphors because this material has very low phonon energy and thus the quenching of the excited state of the lanthanide ions will be minimal. Among the available trivalent rare earth ions, $Dy^{3+}$ is considered as a suitable sensitizer ion because of its special energy levels and long excited level lifetime. In order to identify the photoluminescence properties of rare earth cation doped $La(OH)_3$ nanoparticles, rare earth cations were doped in various percentages (2, 5 and 10 wt. %).

## II. EXPERIMENTAL

Nanocrystalline lanthanum hydroxide powder was prepared by combustion synthesis using high purity lanthanum nitrate as oxidant and citric acid as fuel. Requisite quantities of lanthanum nitrate and citric acid monohydrate were mixed, in the desired fuel to oxidant ratio (F/O=1). Finally ammonia solution was slowly added to adjust the pH at 7. Beaker containing starting precursor was placed over the hot plate and the water solution was left to evaporate at 80 $^{o}$C with continuous mechanical stirring, until a sticky gel was obtained. In order to carry out the gel decomposition, the beaker was transferred to a furnace capable heating above 200$^{o}$C. When the temperature was raised gradually, the decomposed gel got self-ignition around 180$^{o}$C. The spontaneous combustion lasted for about 10-20s and gave the desired powder products. As-prepared powders were then annealed at 800 $^{o}$C for three hours in a muffle furnace to remove the traces of residual reactants and left over carbonaceous matter. Dysprosium doped Lanthanum hydroxide nano particles were prepared by mixing lanthanum nitrate and dysprosium nitrate for three different doping concentrations 2, 5 and 10 wt. %. Prepared samples were named respectively $La(OH)_3$, $La(OH)_3$:Dy-1, $La(OH)_3$:Dy-2 and $La(OH)_3$:Dy-3 for the pure and doped samples.

The crystal structure of pure and $Dy^{3+}$ doped lanthanum hydroxide powders were characterized by an X-ray diffractometer with CuKα radiation (PANAlytical, X'pert Pro). Optical absorption measurements have been performed in a UV-Vis spectrophotometer having a resolution of 0.05 nm (Varian, Cary 5000). Photoluminescence measurements were carried out using Spectro-flurometer (Jobin Yvon Spex FluoroMax-3), where a Xe lamp was employed as the excitation source. The decay time profiles were measured on a Fluorocube spectrophotometer (JOBIN-VYON M/S) with a pulsed-Diode excitation sources and a nano-LED.

## III. RESULTS AND DISCUSSION

### A. *Structural Analysis*

Fig. 2 shows the X-ray diffraction patterns of the pure and dysprosium doped lanthanum hydroxide nanopowder samples. From the diffraction peaks presented in the figure, it can be confirmed that the obtained samples have polycrystalline structures, and are perfectly indexed to the hexagonal crystals of $La(OH)_3$ [space group: P63/m (176)] based on the JCPDS standards (JCPDS cards (No. 36-1481). Within the XRD detection limit, no secondary phases related to hydroxides or oxides of Dy are detected, indicating that the Dy doping does not change the hexagonal structure of $La(OH)_3$ even after doping to a level of 10 wt. %. It implies that the $Dy^{3+}$ doping most probably occur by substituting lanthanum atom in the crystal structure.

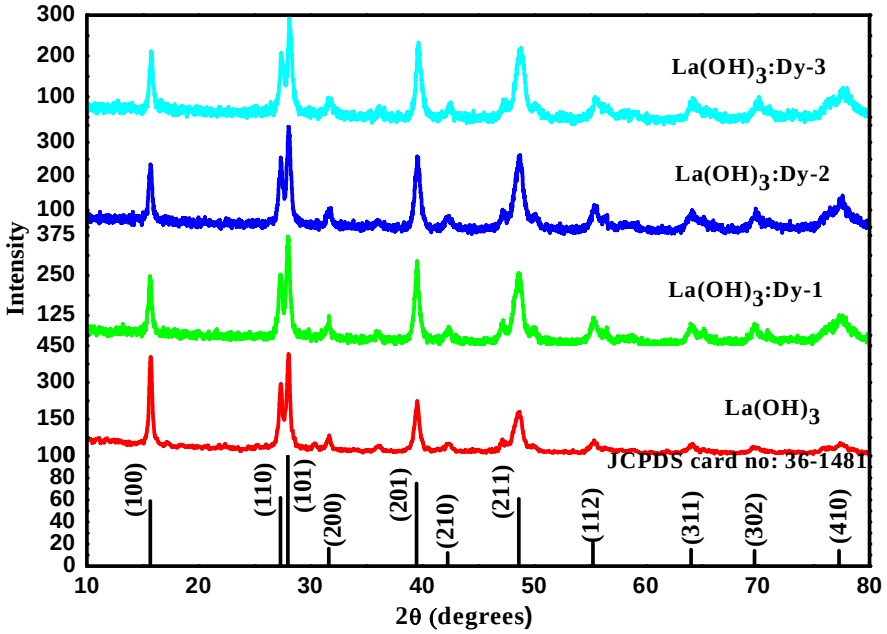


Fig. 2 XRD pattern of pure and Dysprosium ($Dy^{3+}$) doped $La(OH)_3$ nano particles in various concentrations

However, the peak intensities decrease with the increase in doping concentrations, which indicates that an increase in doping concentration deteriorates the crystallinity of the nano particles. This observation further suggests that the present doping level of Dy in $La(OH)_3$ lattice not completely collapse the crystal structure of host material. Since the size of the $Dy^{3+}$ ions is smaller (1.083 Å) compared to $La^{3+}$ (1.36 Å), without much difficulty they occupy the places where $La^{3+}$ ions are present. This can be seen from the shift in the peak positions of the XRD patterns. Reduction in peak height with dopant concentration reveals the reduction in crystallinity of the dopant samples. The increase of FWHM with dopant concentration implies the reduction in particle size on replacing the native ions. On doping, the structural parameters vary with doping concentrations which is listed in Table 1.

Table 1: Structural Parameters of pure and $Dy^{3+}$ doped $La(OH)_3$ nanoparticles from XRD data

| Samples | Lattice parameters Å | Unit cell Volume (V) $Å^3$ | Particle size (D) nm | Density (ρ) $g/cm^3$ | Surface area(S) $x10^6\ cm^2/g$ | Microstrain (ε) $(10^{-3})$ |
|---|---|---|---|---|---|---|
| $La(OH)_3$ | a=6.524 c=3.853 | 142.00 | 24.24 | 4.441 | 0.5574 | -0.150 |
| $La(OH)_3$:Dy-1 | a=6.519 c=3.866 | 142.25 | 31.97 | 4.444 | 0.4223 | 0.184 |
| $La(OH)_3$:Dy-2 | a=6.521 c=3.854 | 141.91 | 28.42 | 4.471 | 0.4722 | -0.135 |
| $La(OH)_3$:Dy-3 | a=6.531 c=3.827 | 141.35 | 25.58 | 4.516 | 0.5194 | -0.832 |
| Standard | a=6.529 c=3.859 | 142.44 | | 4.428 | | |

It is observed from Table 1 that the dopant Dy ions diffuse into the lattice, replacing La ions and due to the mismatch between the ionic radii, the lattice constant and crystallite size slightly deviates from the pure $La(OH)_3$ sample. Density of the Dy doped samples gradually increases with doping concentrations, which confirms the impregnation of the $Dy^{3+}$ ions replacing the native $La^{3+}$ ions. Dysprosium ion reduces the unit cell volumes, particle size on doping and therefore surface area increases in the prepared nanoparticles. Density of the material changes according to the changes in unit cell volume and the microstrain also vary with crystallite size. On doping $La(OH)_3$ with doping concentration 10 wt. % of dysprosium, microstrain attains the maximum value of about $-0.832x10^{-3}$. As the occupancy of $Dy^{3+}$ ions increases, compressive stress along the c-axis of the crystal also increases that makes the crystal more strained.

*B. Optical Studies*

The optical absorption spectra of pure and $Dy^{3+}$ doped $La(OH)_3$ nano powders have been recorded to understand the type of optical transition and to estimate the optical band gap energy. Fig. 3 shows the optical absorption spectra of the pure and $Dy^{3+}$ doped $La(OH)_3$ nano particles.

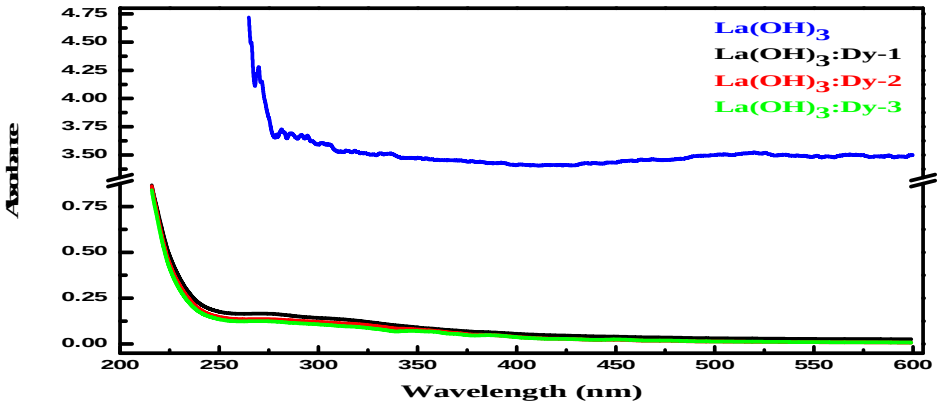


Fig. 3 Optical absorption spectra of the pure and $Dy^{3+}$ doped $La(OH)_3$ nano particles

The relation between absorption coefficient ($\alpha$) and incident photon energy ($h\nu$) can be determined using the well known Tauc's relations [17, 18]; $\alpha = A(h\nu - E_g)^P$ (1)where, 'h', 'A', 'α', 'ν' and '$E_g$' are the Plank constant, a constant, absorption coefficient, light frequency and band gap respectively. Exponent '*p*' denotes the type of the transition; 'p' may have values 1/2, 2, 3/2 and 3 corresponding to the allowed direct, allowed indirect, forbidden direct and forbidden indirect transitions respectively [19]. The type of transition for both pure and $Dy^{3+}$ doped $La(OH)_3$ nanopowder are allowed direct. Constructed Tauc plots, $(\alpha h\nu)^2$ versus hν from the optical absorption spectral data are shown in Fig. 4.

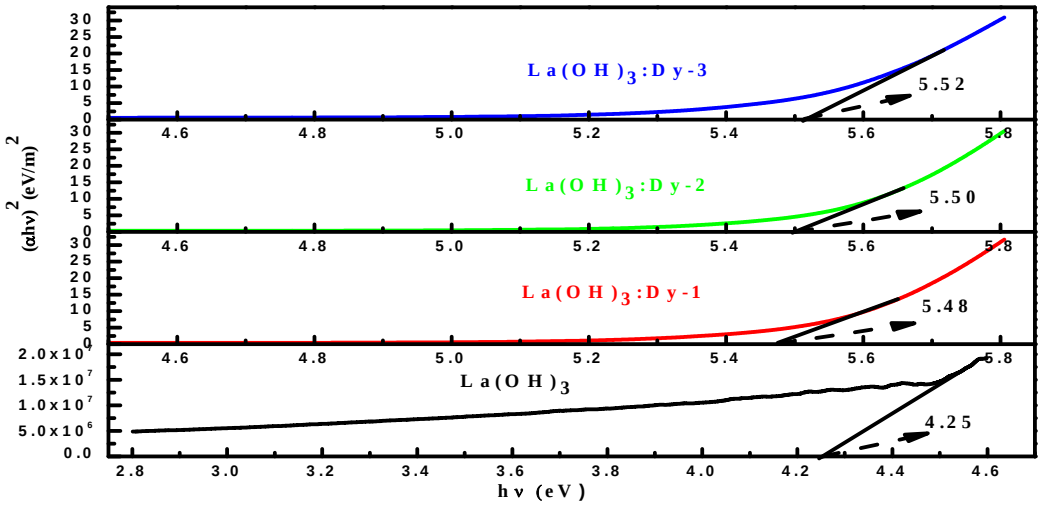


Fig.4 Tauc Plots for the estimation of optical band gap of pure and $Dy^{3+}$ doped $La(OH)_3$ nano particles

Extrapolating the linear portion of the pure $La(OH)_3$ curve yields band gap of 4.25eV, which on doping the band gap changes to 5.48eV, 5.50eV and 5.52eV on increasing the dopant concentrations. It is observed that direct energy band gap increases with the addition of $Dy^{3+}$ ions. The increase in optical energy band gap with the addition of $Dy^{3+}$ may be due to the modified density of localised energy states. The lower the localized states, wider the optical bandgap.

*C. Photoluminescence study*

The electronic configuration of the $Dy^{3+}$ ion is $4f^9$, which gives $^6H$ as the ground state multiplet. The $^6H$ and $^6F$ terms are spin allowed ($\Delta S=0$) where the transitions within the $^6H$ term are also allowed by the orbital angular momentum selection rule $\Delta L = 0$. Hence, these transitions are intense, though they are lying in the infra-red region. When $Dy^{3+}$ ions are excited to the levels above the $^4F_{9/2}$ level there is a fast non-radiative relaxation to this fluorescent level and emission takes place from $^4F_{9/2}$ to its lower levels [20]. Generally, $Dy^{3+}$ ions have two dominant emission bands in the blue (460–500 nm) and yellow (560–600 nm) regions. The blue emission corresponding to $^4F_{9/2} \rightarrow {}^6H_{15/2}$ transition is the magnetic transition, which is insensitive to the local environment, whereas the yellow emission corresponding to $^4F_{9/2} \rightarrow {}^6H_{13/2}$ transition is the hypersensitive electric dipole transition ($\Delta L=2$, $\Delta J=2$) and its intensity is strongly affected by the crystal field around $Dy^{3+}$ ions [21, 22]. Therefore, the color-tunable emissions are expected to be realized in $Dy^{3+}$ ions doped materials by changing the yellow-to-blue intensity ratio[23]. Guo et al. [21] reported that the emission colour of the $Dy^{3+}$-activated $Li_8Bi_2(MoO_4)_7$ phosphors can be changed from yellow to white through modifying the Y/B ratio. Furthermore, Liu et al. [24] also demonstrated that the emission colour of $Dy^{3+}$- activated $NaY(WO_4)_2$ phosphors can be tuned from greenish blue to yellowish green. It is noted that most of the studies on the color-tunable emissions of $Dy^{3+}$ ions were mainly carried out either by adjusting the $Dy^{3+}$ ion concentration or choosing different host lattices. However, there are few investigations on the excitation wavelength dependent emission.

For the measurement of the fluorescence spectrum, a xenon lamp (450W) was used as the excitation light source. The excitation wavelength was 275 nm and the luminescent wavelengths were detected by PMT to a resolution of 0.2 nm. The PL emission spectra of the pure and $Dy^{3+}$ doped $La(OH)_3$ by exciting the samples are shown in Fig. 5. Observed luminescent emission bands at 417 and

492 nm for the pure $La(OH)_3$ nanopowders are corresponding to the typical blue band of $La^{3+}$ ions, respectively, to the $^5D_3 \rightarrow {}^7F_j$ (j = 3–6). Usually $La^{3+}$ does not have any luminescence because of the zero electrons in the 4f shell, and La cannot be regarded as an emission centre and cannot radiate light from the inner atomic 4f shell when crystalline $La(OH)_3$ is formed without impurity and trap centers [25, 26]. The emission of 417 and 492 nm could not contribute to the transition from the conduction band to the valence band. The emission does not originate from a transition between the conduction and valence band; it comes from a deep-level or trap-state emission. Similar results can be found in the reference by Wang [25].

$Dy^{3+}$ doping initiated several photoluminescence peaks extending over green to NIR regions have been observed. This may be due to the transitions from various energy levels of the dopant $Dy^{3+}$ ions. The energy level diagram for the $Dy^{3+}$ ion is shown in Fig. 6. The energy separation from the $^6H_{9/2}$ level to the next lower $^6H_{11/2}$ level is 1900 $cm^{-1}$, which is a small value relative to the nominal phonon energies for oxides. However, $OH^-$ groups have a large phonon energy, which is typically more than 3000 $cm^{-1}$ for various stretching modes. If $OH^-$ or $O^{-2}$ groups coordinate to the $Dy^{3+}$ ions in a solid, they would quench the emission from the $^6H_{9/2}$ level by multi-phonon relaxations. Even then observed photo luminescent peaks are due to transitions between the various energy levels of the dopant ions.

On increasing the dopant concentrations, the emission intensity decreases. The emission spectrum of $Dy^{3+}$ doped $La(OH)_3$ nano-phosphor has been recorded in range of 350–675nm while excitation was given at 275 nm. Generally, $Dy^{3+}$ ion exhibits the detectable transitions below 600nm and the spectrum contains several transitions which can be assigned to the different electronic transitions of $Dy^{3+}$ ions.

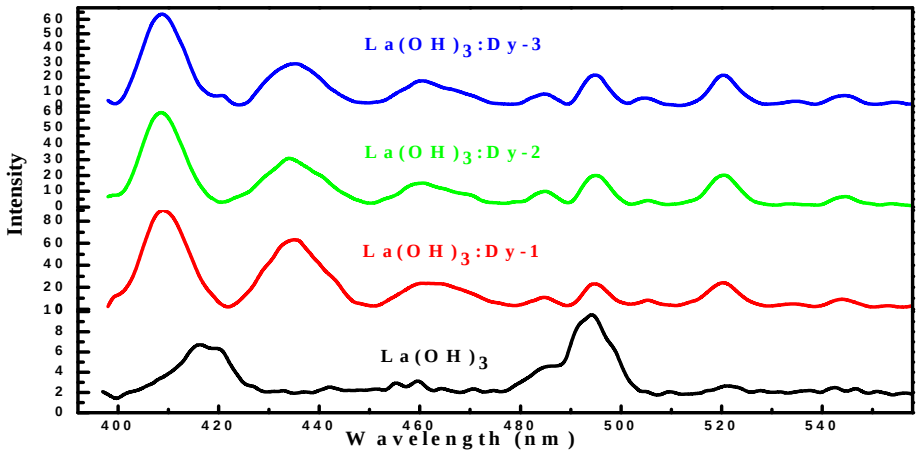


Fig. 5 PL spectra of the pure and $Dy^{3+}$ doped $La(OH)_3$ nano particles.

Two strong emission bands centred at 409 and 435 nm are observed due to the $Dy^{3+}$ transition from the $^6H_{9/2}$, $^6F_{11/2}$ level to the $^6H_{15/2}$ level. Observed peaks in the wavelength range 462, 485, 495, 505, 520, 544, 569, and 592nm are due to transitions between the various energy levels of the dopant ions. Obtained emission spectrum contains the characteristic transition line of $Dy^{3+}$ at 462, 485, 495, 505, 520, 544 nm ($^4F_{9/2} \rightarrow {}^6H_{15/2}$) corresponding to the magnetic dipole transition and at 569 and 592 nm ($^4F_{9/2} \rightarrow {}^6H_{13/2}$, dominated) ($\Delta L = 2$, $\Delta J = 2$), ascribed to electric dipole transition. On varying the doping concentration, the emission peak shifts to lower wavelength side and the peak intensity also decreases with increase of dopant concentration.

The electric dipole transition at 592 nm belongs to hypersensitive transitions, it is very sensitive to the structural environment and influenced strongly by the outside surroundings, hence the $Dy^{3+}$ ions in the $La(OH)_3$ host lattices can serve as a very efficient and sensitive structural probe. The magnetic dipole transition at 462 nm is insensitive to the structural changes. The asymmetric (or yellow to blue, Y/B) ratios indicate that the yellow emission at 592 nm ($^4F_{9/2} \rightarrow {}^6H_{13/2}$) is most important in $Dy^{3+}$ doped $La(OH)_3$ nanocrystals.

Up conversion can also reduce the efficiency when the desired excited state is depleted by cross relaxations or excited state absorption. However, NIR and green emission of the phosphor confirmed the presence of up-conversions. $Dy^{3+}$ in $La(OH)_3$ host lattice emits light from blue to red region. The luminescence comes from the $^4F_{9/2}$ level of dysprosium. The most intensive is a yellow greenish emission, which is assigned to the $^4F_{9/2} \rightarrow {}^6H_{13/2}$ transition.

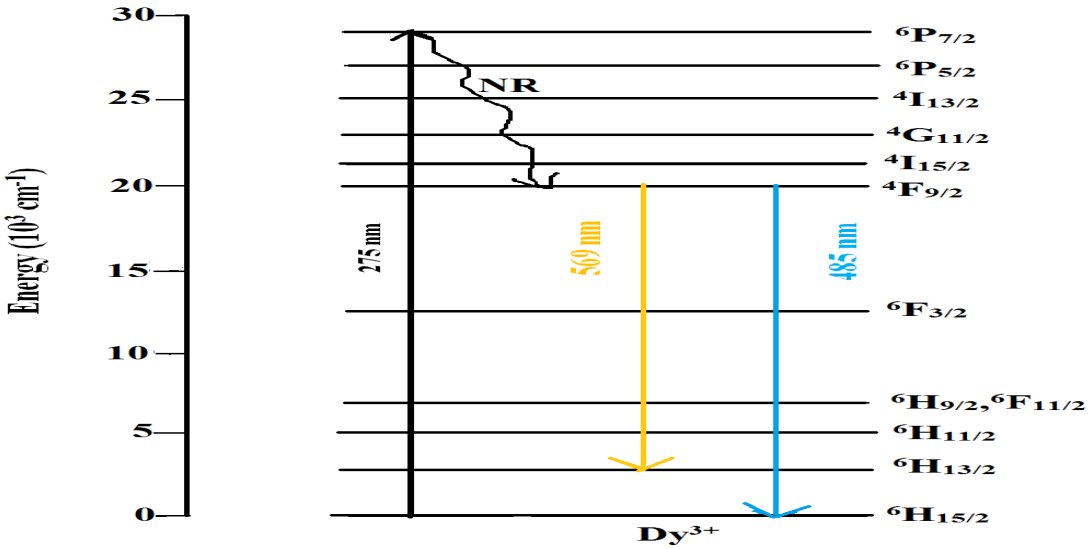


Fig. 6 The energy level diagram of the $Dy^{3+}$ ion

*D. Fluorescence lifetime measurement*

A more accurate estimation of concentration quenching and energy transfer is an emission lifetime measurement. The time resolved fluorescence lifetime measurement was performed to find the fluorescence lifetime of pure and $Dy^{3+}$ doped $La(OH)_3$ nanoparticles. Luminescent decay curves and corresponding fitted curves are depicted in Fig. 7, which represent the decay time of 331nm emission (excited at 295nm) corresponding to the transitions of $La^{3+}$ ions in $La(OH)_3$ nanoparticles. Local phonon energy influences luminescent properties of $Dy^{3+}$ such as intensity, lifetime, and quantum efficiency.

The fluorescence lifetime is calculated by fitting a single exponential function:

$$I = I_0 \exp\left(-\frac{t}{\tau}\right) \qquad (2)$$

where, '$I_0$' is the initial emission intensity at t = 0 and '$\tau$' is the lifetime of the particular level.

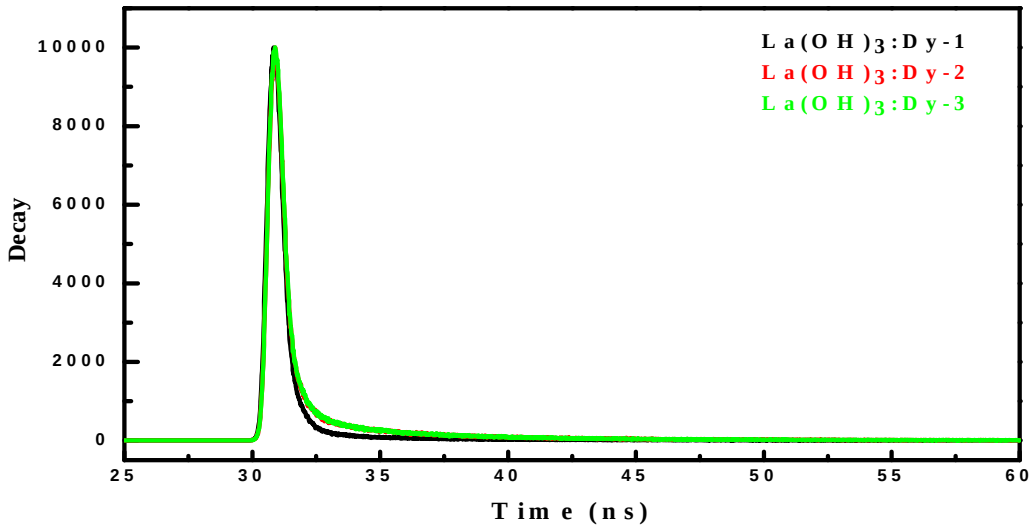


Fig. 7 Luminescent decay curves of $Dy^{3+}$ doped $La(OH)_3$ nano particles

The obtained luminescent lifetime of $Dy^{3+}$ doped $La(OH)_3$ nanopowders is 4.47, 5.08 and 5.13ns for the three doping concentrations. It can be found that the luminescent lifetime gets longer when the doping concentration increases. This is attributed to surface state recombination of electron-hole pairs [27, 28].

## IV. CONCLUSION

The pure and $Dy^{3+}$ doped $La(OH)_3$ phosphor has been synthesized through auto-combustion method. From the XRD pattern, no structural changes were found upon incorporation of $Dy^{3+}$ into the host lattice in all cases confirming good solubility of the dopant. The optical properties were also modified with $Dy^{3+}$ incorporation; the band gap increased by doping. It is obvious that the doping concentration has significant effect on the luminous intensity of emission. Most of the peak intensity decreases on increasing the doping concentrations. This may be due to incorporation of more amounts of dopant ions that spoils the lattice structure partly as evidenced from the XRD studies. The lifetime of increases in presence of $Dy^{3+}$ ions, this favors to give large emission intensity. Thereby, $Dy^{3+}$ doped $La(OH)_3$ could be an excellent candidate for white light emitting diodes devices.

## REFERENCES

[1] Yen W M, Shionoya S, Yamamoto H 2006 Practical Applications of Phosphors, CRC Press.
[2] Singh S K, Singh A K, Kumar D, Prakash O and Rai S B Efficient UV–visible up-conversion emission in $Er^{3+}/Yb^{3+}$ co-doped $La_2O_3$ nano-crystalline phosphor 2010 Appl. Phys. B.98 173-179.
[3] Park J, Park S,Kim C,Park H and Choi S 2001 Photoluminescence properties of the $Eu^{3+}$ in $La_2O_3$ J. Mater. Sci. Lett. 20 2231-2232
[4] Adachi G, Imanaka N and Kang Z 2004 Binary Rare Earth Oxides, Kluwer Academic Publishers, Amsterdam
[5] Shannon R D 1976 Revised effective ionic radii and systematic studies of interatomic distances in halides and chalcogenides Acta Cryst. A. 32 751-767.
[6] Lide D R. CRC Handbook of Chemistry and Physics, 87thedition, CRC Press, pp. 9-77.
[7] Pandey A and Rai V K 2012 Colour emission tunability in $Ho^{3+}$–$Tm^{3+}$–$Yb^{3+}$ co-doped $Y_2O_3$ upconverted phosphor Appl. Phys. B. 109 611-616.
[8] Liu X, Yan L and Zou J Tunable Cathodoluminescence Properties of $Tb^{3+}$-Doped $La_2O_3$Nanocrystalline Phosphors 2010 J. Electrochem. Soc. 157 (2) P1-P6
[9] H. Q. Liu, L. L. Ying, and S. G. Chen, 2007 Effect of $Yb^{3+}$ concentration on the upconversion of $Er^{3+}$ ion doped $La_2O_3$ nanocrystals under 980 nm excitation Mater. Lett. 61 (17) 3629–3631
[10] Auzel F Upconversion and Anti-Stokes Processes with f and d Ions in Solids2004 Chem. Rev. 104 139-173
[11] Sivakumar S, van Veggel F C J M and May P S Near-Infrared (NIR) to Red and Green Up-Conversion Emission from Silica Sol−Gel Thin Films Made with $La_{0.45}Yb_{0.50}Er_{0.05}F_3$ Nanoparticles, Hetero-Looping-Enhanced Energy Transfer (Hetero-LEET): A New Up-Conversion Process,2007 J. Am. Chem. Soc. 129(3) 620-625
[12] Milliez J, Rapaport A, Bass M, Cassanho A and Jenssen H P High-brightness white-light source based on up-conversion phosphors 2006 J. Disp. Technol. 2 307-311.
[13] Capobianco J A, Vetrone V, Boyer J C, Speghini A and Bettinelli M Visible upconversion of $Er^{3+}$ doped nanocrystalline and bulk $Lu_2O_3$ 2002 Opt. Mater. 19 259-268
[14] Mao Y B, Tran T, Guo X, Huang J Y, Shih C K, Wang K L and Chang J P Luminescence of nanocrystalline erbium-doped yttria, 2009 Adv. Funct. Mater.19 748-754.
[15] Chen D Q, Wang Y S, Zheng K L, Guo T L, Yu Y L and Huang P Bright upconversion white light emission in transparent glass ceramic embedding $Tm^{3+}/Er^{3+}/Yb^{3+}$:β-$YF_3$ nanocrystals 2007 Appl. Phys. Lett. 91 251903.
[16] Sivakumar S, Frank C. J. M van Veggel and Raudsepp M Bright White Light through Up-Conversion of a Single NIR Source from Sol−Gel-Derived Thin Film Made with $Ln^{3+}$-Doped $LaF_3$ Nanoparticles 2005 J. Am. Chem. Soc.127 12464-12465.
[17] Osuwa J C, Oriaku C I and Atuloma C M Study of physical properties of ternary $Cu_{1.1}Cd_{4.0}S_{4.9}$ thin film glasses 2010 Chalcog. Lett.7 383-38
[18] Pankove J I 1971 Optical Processes in Semiconductors Prentice-Hall, New Jerc
[19] Hagfeldt A and Gratzel M Light-Induced Redox Reactions in Nanocrystalline Systems1995 Chem. Rev. 1995, 95, 49-68.
[20] Ch.Basavapoornima, Jayasankar C K and Chandrachoodan P P Luminescence and laser transition studies of $Dy^{3+}$:K–Mg–Al fluorophosphate glasses 2009 Physica B Condens Matter. 404 235-242.
[21] Zhao J, Guo C, Su X, Noh H M and Jeong J H Electronic Structure and Luminescence Properties of Phosphor $Li_8Bi_2(MoO_4)_7$: $Dy^{3+}$ 2014 J. Am. Ceram. Soc. 97 1878-1882.
[22] Tian Y, Chen B, Tian B, Hua R, Sun J, Cheng L, Zhong H, Li X, Zhang J, Zheng Y, Yu T, Huang L and Meng Q Concentration-dependent luminescence and energy transfer of flower-like $Y_2(MoO_4)_3$:$Dy^{3+}$ phosphor 2011 J. Alloys Compd. 509 6096-6101
[23] Su Q, Pei Z, Chi L, Zhang H, Zhang Z and Zou F The yellow-to-blue intensity ratio (Y/B) of $Dy^{3+}$ emission 1993 J. Alloys Compd. 192 25-27.
[24] Liu X, Xiang W, Chen F, Hu Z and Zhang W Synthesis and photoluminescence characteristics of $Dy^{3+}$ doped $NaY(WO_4)_2$ phosphors 2013 Mater. Res. Bull. 48 281-285
[25] Hu C G, Liu H, Dong W, Zhang Y Y, Bao G, Lao C S and Wang Z L La(OH)3 and La2O3 Nanobelts—Synthesis and Physical Properties, 2007 Adv. Mater. 19 470-474
[26] Li J Y 2003 Luminescent Materials of Rare Earths and Their Applications (Beijing: Chemical Industry), p 8
[27] Wilcoxon, J P, Samara G A and Provencio P N Optical and electronic properties of Si nanoclusters synthesized in inverse micelles 1999 Phys. Rev. B. 60 2704-2714.
[28] Lu X, Hanrath T, Johnston K P and Korgel B A Growth of Single Crystal Silicon Nanowires in Supercritical Solution from Tethered Gold Particles on a Silicon Substrate 2003 Nano. Lett. 3 93-99

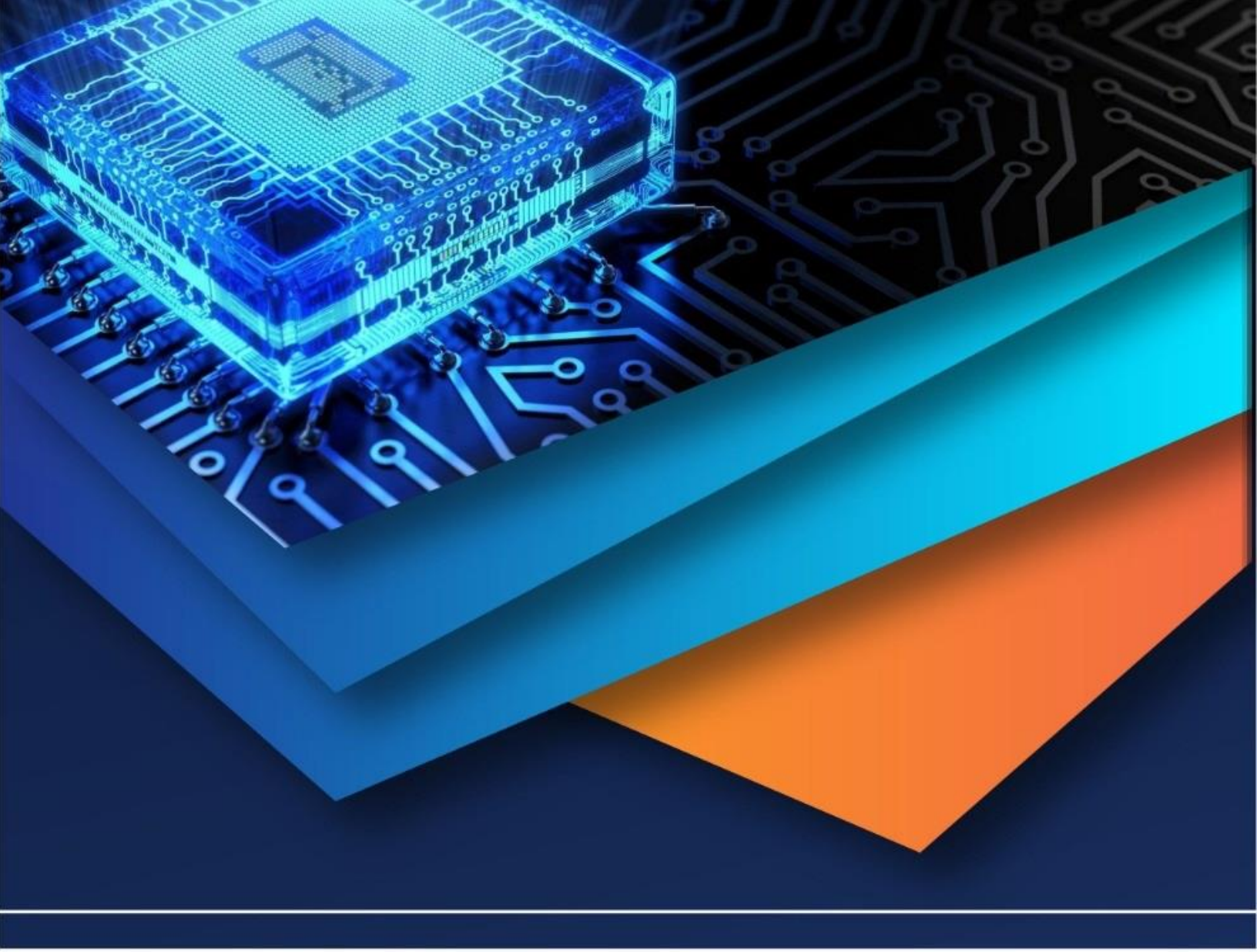

10.22214/IJRASET

45.98

IMPACT FACTOR: 7.129

IMPACT FACTOR: 7.429

# INTERNATIONAL JOURNAL FOR RESEARCH

IN APPLIED SCIENCE & ENGINEERING TECHNOLOGY